MATERIAL MODELLING AND IMPACT ANALYSIS OF POLYURETHANE FOAM FILLED T_2O TRANSPORTATION PACKAGES

R.G. SAUVÉ, W.W. TEPER, G.J. SULLIVAN
Nuclear Systems Department,
Ontario Hydro,
Toronto, Ontario,
Canada

Abstract

MATERIAL MODELLING AND IMPACT ANALYSIS OF POLYURETHANE FOAM FILLED T_2O TRANSPORTATION PACKAGES.

Packages used in the road transportation of tritiated heavy water (T_2O) must demonstrate the ability to withstand severe shocks and impacts, such as those prescribed by IAEA Regulations. The paper describes part of the analytical assessment of a proposed package design to determine its structural integrity under impact conditions resulting from postulated accidents. The focus of the work described is on the mathematical modelling of the polyurethane foam used in the sandwich construction of the overpack and on the development of acceptance criteria to evaluate the design. Versions of the computer codes DYNA3D and HONDO incorporating these material models were utilized in performing the numerical computation. Comparison of the predicted results of a punch drop with those of experiments show excellent agreement. Results of the 1 m punch drop and the 9 m edge drop on the lid end are presented. The proposed design meets the specified acceptance criteria, thus demonstrating it will retain its structural integrity under the impact conditions imposed.

1. INTRODUCTION

Packages used in the road transportation of low level radioactive wastes, such as tritiated heavy water (T_2O), must demonstrate the ability to withstand severe impacts such as those prescribed by IAEA Regulations. Ontario Hydro has undertaken a programme to design, license and build such a prototype package. The purpose of the present study [1] is to evaluate the design in order to determine its structural integrity under impact conditions resulting from the following postulated cases: (a) a 1 m punch drop onto a mild steel pin; (b) a 9 m lid-down, flat-end drop onto an unyielding target surface; (c) a 9 m edge drop of the lid end onto an unyielding target surface. As shown in Fig. 1, the tritiated heavy water transportation package (THWTP) comprises a cylindrical T_2O container and an overpack of sandwich construction with 304L stainless steel inner and outer shells with a polyurethane foam core. The total weight of the container, including the 12 000 lb payload, is 36 700 lb.[1] The primary containment boundary is located at the overpack inner housing, overpack lid and outer containment seals in the lid region.

[1] 1 lb = 0.4536 kg.

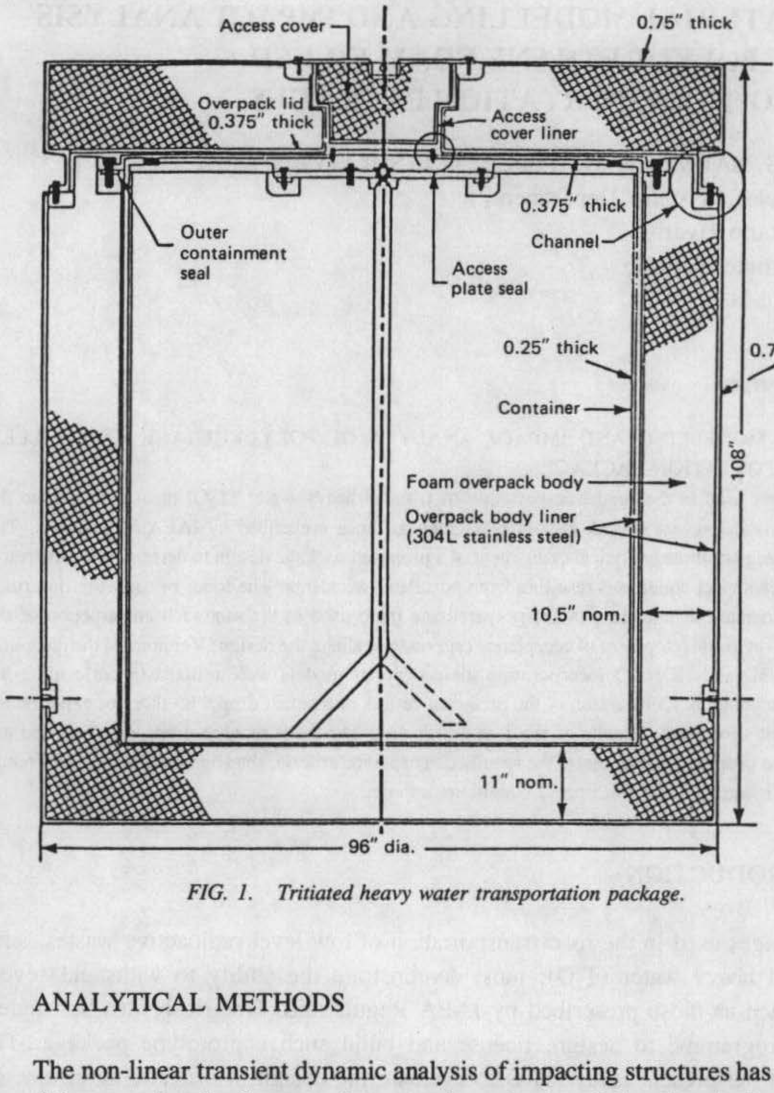

FIG. 1. Tritiated heavy water transportation package.

2. ANALYTICAL METHODS

The non-linear transient dynamic analysis of impacting structures has long been one of the more involved areas of structural mechanics. It involves both non-linear geometric and material behaviour affecting wave propagation in two- and three-dimensional continuums. A two-material structure, such as the THWTP, where steel and polyurethane foam interface, further complicates the problem. Owing to the inherent complexity of the problem, the finite element method was applied in the form of two computer codes: HONDO [2] for axisymmetric analysis and DYNA3D [3, 4] for three-dimensional analysis. Both of these computer codes are based on the Galerkin form of the finite element method and are applicable to the large deformation inelastic transient dynamic response of solids. Spatial discretization is achieved using linear isoparametric elements (four-noded quadrilaterals in HONDO and four-, six- or eight-noded elements in DYNA3D).

A number of materials models and equations of state are available to cover a broad range of materials behaviour, including elastic-plastic, soil, soil-structure and explosive-structure interactions. The equations of motion are numerically integrated using a form of the central difference operator. This scheme is explicit and as a result it is conditionally stable with respect to time step size. A continuous monitor of the time step is made throughout the solution to ensure that it is below a critical time step which is required to maintain operator stability. The major differences between the computer codes are in the stress–strain measures used in the material description and the approach used to control 'hourglassing' or zero energy modes. In DYNA3D, the materials model constitutive relations used are specified in terms of true stress and true strain, whereas in HONDO they are specified in terms of the second Piola–Kirchhoff stress and Green–St. Venant strain. A contact–impact algorithm permits gaps and sliding along zone boundaries and material interfaces. These interfaces can be tied to admit variable zoning without the need for transition regions.

Versions of HONDO [2] and DYNA3D [3] have been adapted for use at Ontario Hydro on the Univac 1182/1191 computer facility. Enhancements include run-time user interaction which permits the run to be interrogated for current momentum levels, solution time and time step. Upon completion of the run, these data can then be used to obtain the impact force time history from the derivatives of the momentum time history curves. Pre- and post-processors have been developed which interface with both computer codes for ease of model generation and retrieval of structural deformed plots at selected times, displacement/velocity time history plots and stress–strain measures for comparison with acceptance criteria. Further details of the Ontario Hydro versions and implementation, along with verification cases, are given in Ref. [4].

The loading on the models was obtained in terms of an initial velocity applied to the complete region defining the package, using the following relation from rigid-body mechanics: $V_0 = [2gh]^{1/2}$, where V_0 = initial velocity at impact, h = drop height and g = gravitational constant.

3. MATERIALS MODELS

For the severe impact cases discussed in this analysis, the materials models used must be capable of providing an adequate representation of the moderately large strain regime. This entails a non-linear description of the materials behaviour in the post-yield region in terms of:

(1) A yield criterion to determine the threshold at which plastic flow begins;
(2) A flow rule to relate plastic strain increments with total deviatoric stress components;
(3) A hardening rule to specify the modification of the yield condition during plastic flow;
(4) In the case of polyurethane foam, an equation of state for pressure versus volumetric strain with compaction.

3.1. Stainless steel

Since the 304L SS material is ductile and isotropic, a von Mises' yield criterion is adopted with an isotropic hardening rule. A straight-line approximation is used to represent the strain-hardening behaviour. The material properties [1] for 304L stainless steel used in the analysis are:

E = modulus of elasticity = 28×10^6 lbf/in^2.[2]
σ_y = yield stress = 44 300 lbf/in^2.
μ = Poisson ratio of 0.27.
E_t = strain-hardening modulus = 3.5×10^5 lbf/in^2 (true stress–strain), which is equal to 1.0×10^5 lbf/in^2 (second Piola–Kirchhoff stress and Green-St. Venant strain).

3.2. Polyurethane foam

Although data on 304L stainless steel are well documented, those for polyurethane foam are not. Polyurethane foams exhibit a pressure-dependent behaviour. They crush and compact under pressure due to the presence of voids. The model used is based on the work in Ref. [5], which describes a simple, but useful, model for soils and crushable foams whose material properties are not easily characterized. An elementary isotropic plasticity theory is utilized in which a pressure-dependent flow rule is defined as:

$$\phi = J_2 - (a_0 + a_1\sigma_p + a_2\sigma_p^2)$$

where J_2 is the second invariant of the deviatoric stress tensor, σ_p is the hydrostatic stress and a_0, a_1 and a_2 are derived constants. For $\phi \leq 0$, the material is elastic. Tensile fracture occurs when

$$\sigma_p < \text{min root } [a_0 + a_1\sigma_p + a_2\sigma_p^2 = 0]$$

At yield $\phi = 0$, i.e.

$$J_2 = a_0 + a_1\sigma_p + a_2\sigma_p^2 = 1/3\ \sigma_y^2$$

where σ_y is the yield point in uniaxial compression corresponding to σ_p. The values of the constants a_0 and a_1 used in the flow rule are evaluated using the experimental data obtained for the 23 lbf/ft^3 polyurethane foam, described in Ref. [1].

---

[2] 1 lbf/in^2 = 6.895×10^3 Pa.

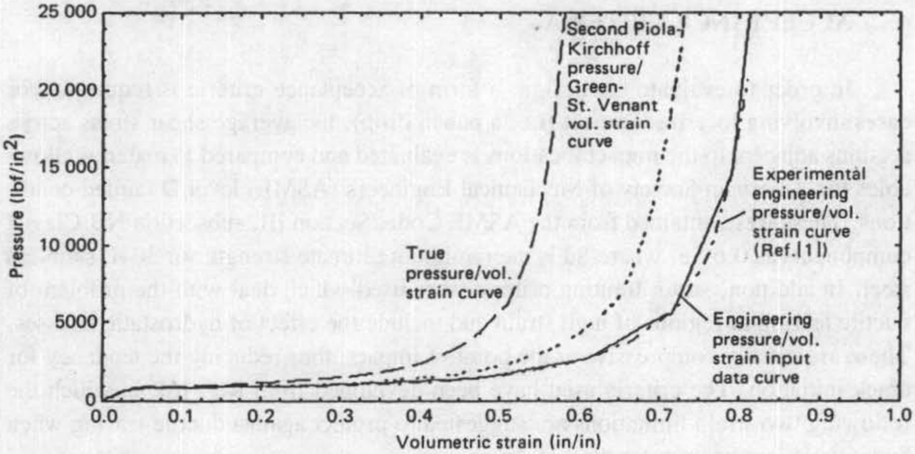

FIG. 2. Pressure–volumetric strain curve for the polyurethane foam model.

As pointed out in Ref. [5], a parabolic curve (i.e. $a_2 = 0$) is utilized, since this fits the data for such materials very well. From the test results, the tensile threshold, that is the pressure at which tensile fracture occurs, is found to be

$$\sigma_{p0} = -223.84 \text{ lbf/in}^2 \text{ (negative denotes tension)}$$

Since the fracture occurs prior to yield, $\sigma_y = 0$. The yield in shear is found from a pure shear test: $\tau_{y1} = 149.4$ lbf/in². The corresponding yield in tension is $\sigma_{y1} = \sqrt{3}\ \tau_{y1} = 258.75$ lbf/in². Since this is a case of pure shear, $\sigma_{pl} = 0$. Substitution leads to

$$a_0 + a_1\sigma_p = \frac{\sigma_y^2}{3}$$

The final equation for the yield stress in terms of hydrostatic pressure is

$$\sigma_y^2 = 3\ (22\ 317.4 + 99.7\ \sigma_p)$$

The volumetric yield is determined by a function which describes the pressure versus volumetric strain behaviour, as shown in Fig. 2, for the various strain measures. Elastic unloading is assumed for a tensile cutoff pressure using an unloading bulk modulus (Fig. 2). If tensile failure occurs, pressure is left at the cutoff value and the deviatoric stress components are zeroed. Note that pressure is positive in compression. The data were input into the computer codes in the form of an equation of state with compaction for the pressure versus volumetric strain relation, constants a_0, a_1 for the pressure-dependent flow rule, an unloading bulk modulus, shear modulus and pressure cutoff.

4. ACCEPTANCE CRITERIA

In order to evaluate the design, a form of acceptance criteria is required. For cases involving localized impact (i.e. a punch drop), the average shear stress across sections adjacent to the impact locations is evaluated and compared to material allowables for American Society of Mechanical Engineers (ASME) level D faulted conditions. These were obtained from the ASME Code, Section III, subsection NB Class I components as 0.6 Su, where Su is the minimum ultimate strength for 304L stainless steel. In addition, strain limiting criteria were used which deal with the problem of ductile tearing in regions of high strain and include the effect of hydrostatic stresses. These are usually compressive at the point of impact, thus reducing the tendency for crack initiation. The criteria used have been developed from Ref. [6], in which the following two strain limitations are suggested to protect against ductile tearing when hydrostatic stresses are tensile:

(1) For membrane strains: $\epsilon_m \leq 0.7$ Zn.

(2) For peak strains ϵ_{pk}:

$$\epsilon_{pk} \leq 0.7 \frac{\sinh\left[\frac{\sqrt{3}}{3}(1-n)\right]}{\sinh\left[\frac{\sqrt{3}}{3}(1-n)(TF)\right]} \epsilon_f \quad \text{(for terms in [ ] > 0.2)}$$

$$\epsilon_{pk} \leq 0.7\,[0.2]\,\epsilon_f \quad \text{(for terms in [ ] } \leq 0.2\text{)}$$

where ϵ_f is the true strain at fracture in uniaxial tension

TF is the triaxiality factor $= \left(\frac{\sigma_1 + \sigma_2 + \sigma_3}{\bar{\sigma}_f}\right)$

$\bar{\sigma}_f$ is the effective von Mises' stress

n is the strain-hardening exponent in the equation $\bar{\sigma} = A\,(B + \bar{\epsilon})^n$, which approximates the true stress–strain curve (i.e. n= 0.5 for stainless steel, n = 0.2 for carbon steel)

Z is ϵ_{max}/n.

Values of maximum strain at failure (ϵ_{max}) are readily available for some simple cases: uniaxial tension $\epsilon_{max} = n$, pressurized cylinder $\epsilon_{max} = 0.577$ n, pressurized sphere $\epsilon_{max} = 0.677$ n. For other geometries and loading conditions, the effective strain must be derived from the plastic instability condition ($\partial P/\partial\epsilon = 0$). This may present substantial difficulty when dealing with complex strain distributions, or it may necessitate some conservative evaluation of the allowable effective strain. Using the above approach, allowables for peak and membrane strains for the THWTP stainless steel shells, when the hydrostatic stresses are tensile, are obtained assuming a predominant biaxial stress distribution as follows: The allowable membrane strain = $0.7 \times 0.577 \times 0.5 = 0.20$ (20%). The allowable peak strain = $0.7 \times \epsilon/\epsilon_f \times 0.5$ ($\epsilon_f = n = 0.5$). From Ref. [6] a value for ϵ/ϵ_f in a biaxial stress state is 0.665. Thus, the allowable peak strain = $0.7 \times \epsilon/\epsilon_f \times 0.5 = 0.23$ (23%). Since the outer package is not a primary containment boundary, the full absorbing capability of the structure is taken so that the allowable membrane strain is 28% and the allowable peak strain is 33%.

In order to apply these limits, some interpretation of the analytical results is necessary. In the work described herein, the effective plastic strains and effective

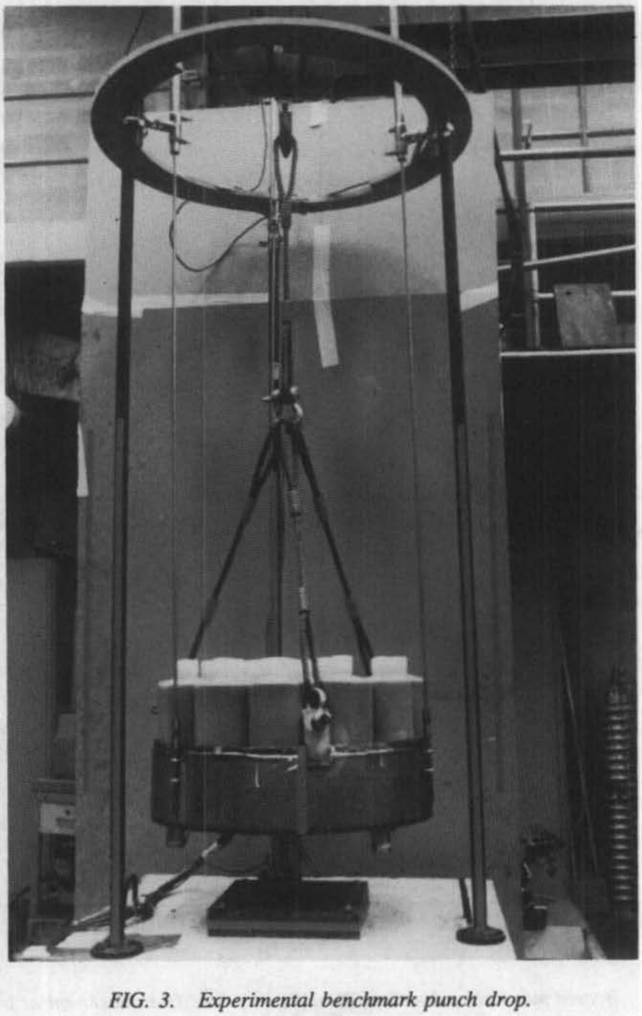

FIG. 3. Experimental benchmark punch drop.

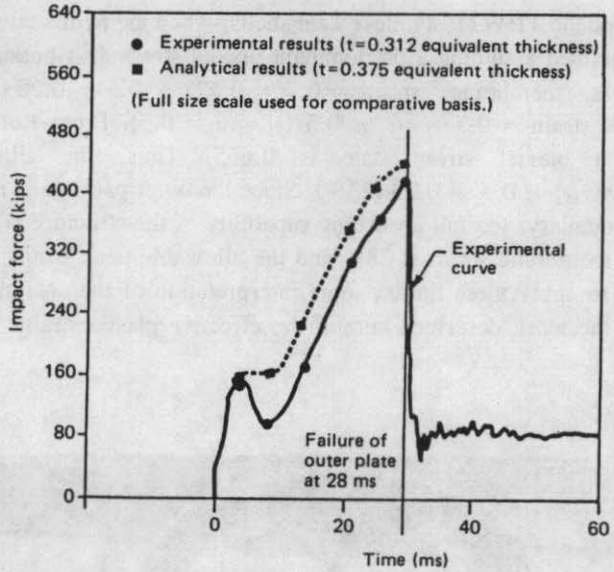

FIG. 4. Bottom punch drop benchmark/verification case (total impact force-time history, comparison). (1 kip is equivalent to a 453.6 kg load; ksi = kips per square inch.)

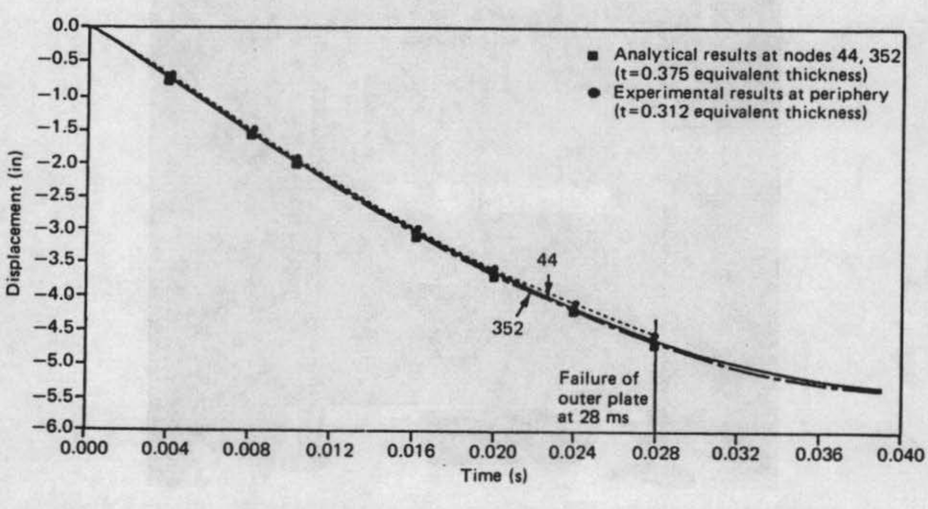

FIG. 5. Bottom punch drop benchmark/verification case (z-displacement at periphery).

stresses in the stainless steel are obtained across selected sections of the finite element model. The resulting average and peak strains are obtained for elements whose hydrostatic stress component is tensile and then compared to the allowable strain limits.

5. BENCHMARK/VERIFICATION CASE

In order to demonstrate the validity of the analytical models and provide some insights into the expected error bounds, a benchmark test using an experimental ¼-scale model was performed. Apart from scale, the model differs from the prototype design only in the thickness of the outer shell, which is reduced in order to provide for a failure in punching shear. This enabled a benchmark of failure limits in order to confirm their conservatism. The experimental setup [1], shown in Fig. 3, consists of a 48 inch drop onto a 6 inch diameter mild steel pin.[3] Owing to the localized nature of this drop, only the lower portion of the overpack is considered with the remaining weight of the package plus contents included as a non-structural mass. The comparisons between experiment and analytical predictions are given in terms of impact force and displacement time histories, as shown in Figs 4 and 5, respectively. The comparisons incorporate the applicable scaling laws and use the full scale as the comparative basis. As seen in Figs 4 and 5, good correlation is obtained.

From the allowables for punching shear given in Section 4, the limit is obtained as 42 ksi based on a minimum ultimate strength of 70 ksi obtained from the ASME code, Appendix F. The benchmark indicates that the ultimate value was approximately 110 ksi, which leads to an allowable in punching shear of 66 ksi, thus demonstrating conservatism in the choice of allowables.

6. PROTOTYPE THWTP IMPACT SIMULATIONS

Once the analytical approach was verified, a series of simulations on the actual prototype THWTP were carried out in accordance with IAEA Regulations. Only a brief description is given here, though further details are given in Ref. [1]. The major assumptions used in the analysis are:

(1) In all the 9 m drop cases, the THWTP is assumed to impact onto an unyielding surface. This is a conservative assumption, since in reality no surface is unyielding. Even small plastic distortions of the target surface result in reduced strains.
(2) To account for the weight of the inner container and payload, an equivalent density is calculated for elements of the overpack at the overpack-to-container surface. They are considered to be non-structural in the analysis.

---

[3] 1 inch = 25.4 mm.

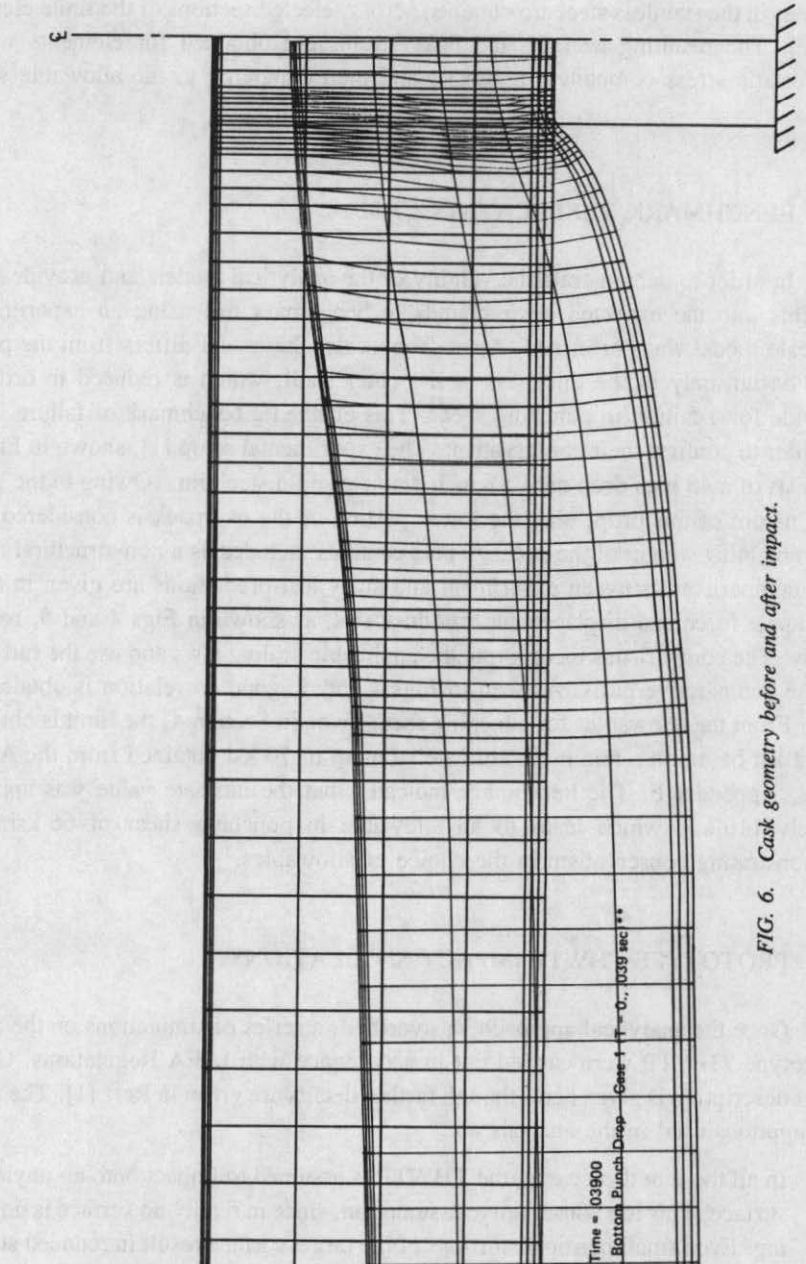

FIG. 6. Cask geometry before and after impact.

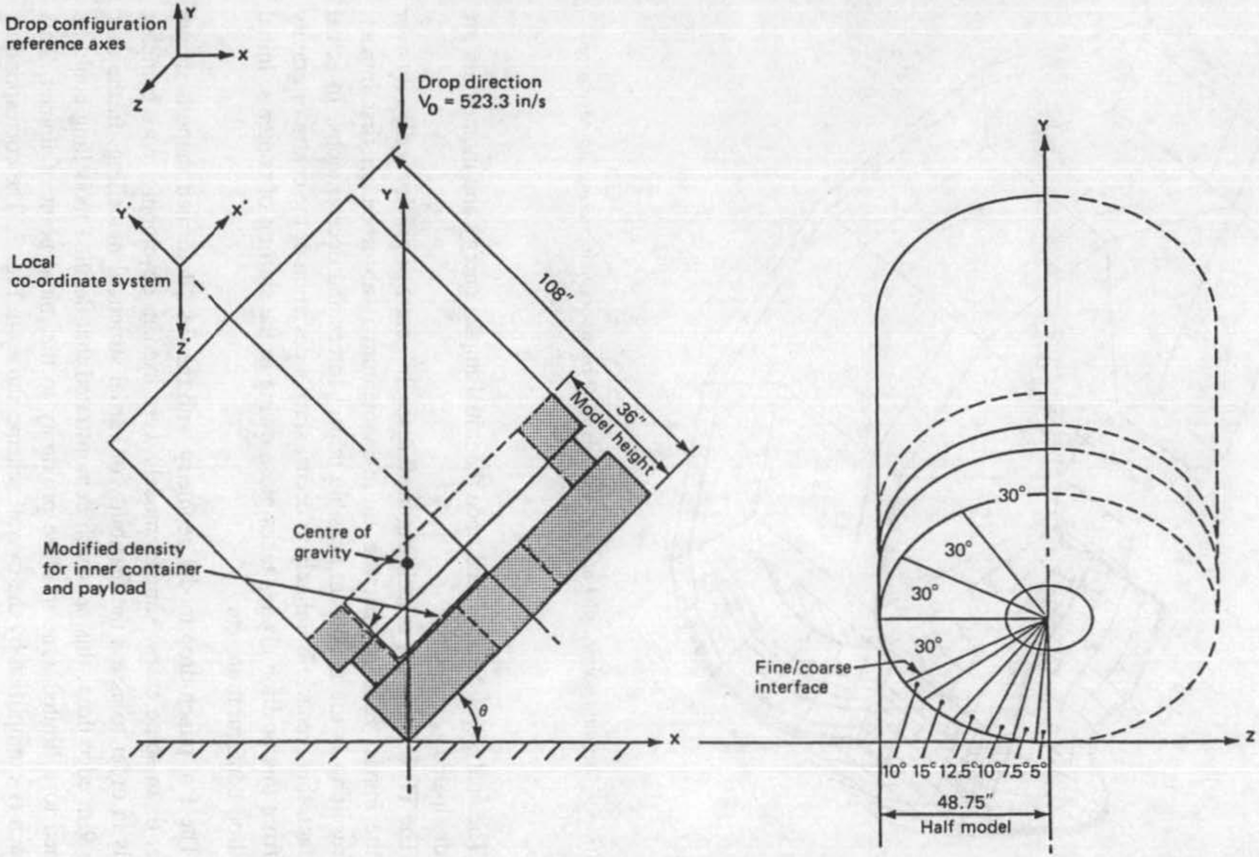

FIG. 7. *Overall modelling considerations for the THWT package (9 m lid edge drop).*

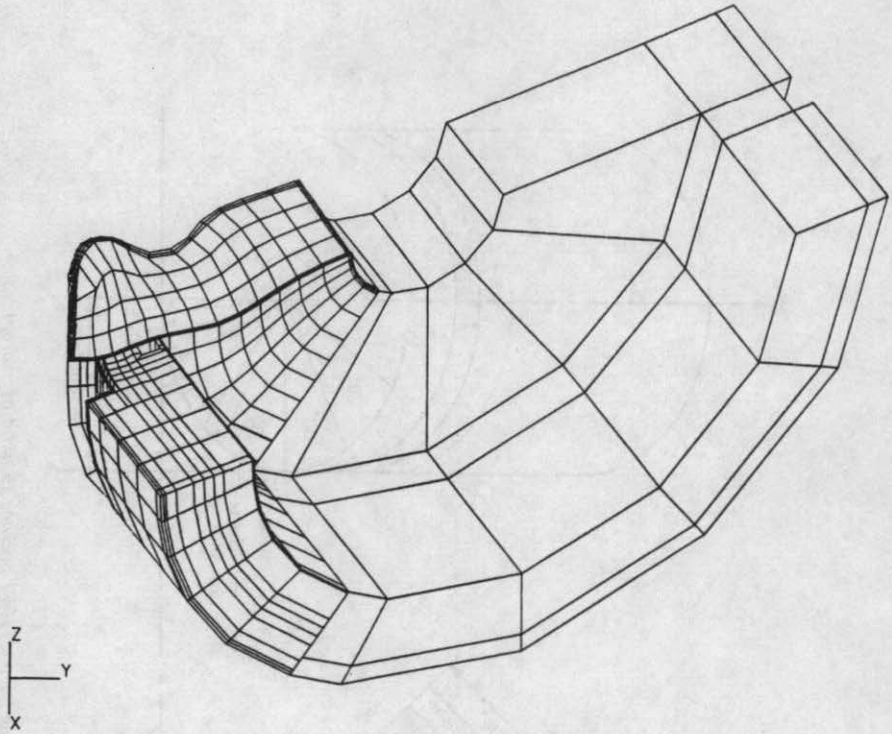

FIG. 8. Overall deformed plot at time = 23 ms (T_2O transportation package lid edge drop).

(3) The analysis is discontinued once the initial impact energy and momentum are dissipated.

(4) The THWTP model is such that in all cases the centre of gravity is directly over the impact zone so that the entire momentum is absorbed on first impact, resulting in the maximum possible impact forces and decelerations. In actual fact, this scenario is unlikely to occur, since a deviation of the centre of gravity from this position always takes place owing to the shifting of contents, initial drop configuration, etc.

The 1 m punch-drop model geometry with the final deformed shape is shown in Fig. 6. In some cases, simpler models were used in developing more complex models in order to assess the feasibility of partial structural modelling. In the case of the 9 m edge drop, this approach demonstrated that detailed modelling could be confined to a limited zone in close proximity to the initial point of impact. This approach is exemplified by the overall scheme shown in Fig. 7. The corresponding computer model of the reduced structure is given in Fig. 8. A typical deformed partial model of the prototype package in the case of an edge drop is also shown in Fig. 8. The maximum decelerations of the package for the various drops are, for a

1 m punch drop: 17g, for a 9m lid flat-end drop: 308g and for a 9 m lid edge-drop: 82g.

The results of the simulations demonstrate that in the critical areas of the prototype package, such as the channel and seal plate area, the effective plastic strains are below the allowables and that the outer shell will resist a 1 m punch drop.

REFERENCES

[1] SAUVÉ, R.G., SULLIVAN, G.J., TEPER, W.W., Analytical Assessment of the Tritiated Heavy Water Transportation Package: Accidental Impact Simulation, Rep. OH-85105, Ontario Hydro, Toronto (1985).

[2] KEY, S., HONDO — A Finite Element Computer Program for the Large Deformation Dynamic Response of Axisymmetric Solids, Rep. SLA-74-0039, Sandia National Lab., Albuquerque, NM (1975).

[3] HALLQUIST, J.O., Theoretical Manual for DYNA3D, Rep. UCID-19401, Lawrence Livermore Natl Lab., Livermore (1983).

[4] SAUVÉ, R.G., SULLIVAN, G.J., Ontario Hydro DYNA3D Computer Code System (Non-Linear Dynamic Analysis of Solids in Three Dimensions), Rep. OH-84108 Ontario Hydro, Toronto (1984).

[5] KRIEG, R.D., A Simple Constitutive Description for Cellular Concrete, Rep. SC-DR-72-0883, Sandia National Lab., Albuquerque, NM (1972).

[6] COOPER, W.E., Rationale for a Standard on the Requalification of Nuclear Class 1 Pressure Boundary Components, Rep. EPRI-NP-1921, Electric Power Research Institute, Palo Alto, CA (1981).